
variability and spectral variation of 3C 66A

Shao Ming Hu^{1,2} • Jianghua Wu³ • H. Y. Guo⁴ •
X. Zhou³ • X. Zhang⁵ • Y. G. Zheng⁵

Abstract 3C 66A was monitored by the BATC (Beijing-Arizona-Taipei-Connecticut) telescope from 2005 to 2008, 1994 observations were obtained on 89 nights. Detailed research and analysis was performed on these observations in this paper. A long term burst occurred in the whole light curve. No intra-day variability was claimed in our campaign by intra-night light curve analysis. Time lag of shorter wavelength preceding longer wavelength was shown by correlation analysis. The results showed that the optical spectral shape turned flatter when the source brightened, and the spectral variability indicator was bigger on shorter time-scale as determined by the color indices variation analysis.

Keywords blazar; variability; photometry; time delay

1 Introduction

3C 66A is a classic blazar object, and blazars are the most extreme subclass of the active galactic nu-

lei. They show highly variable non-thermal continuum emission ranging from radio up to X-ray and often to γ -ray frequencies on different time scales, and they exhibit strong polarization from radio to optical wavelength (e.g., Maraschi et al. 1994; Urry & Padovani 1995; Hartman et al. 1999; Gupta et al. 2004; Raiteri et al. 2008; Villata et al. 2009; Bauer et al. 2009). Blazars can be classified into BL Lac objects (BL Lacs) and flat-spectrum radio quasars (FSRQs), based on their emission line features (Landt et al. 2004). The former one has a featureless optical continuum or has very weak emission or absorption lines, while the latter has some strong and broad emission lines. Studies of broadband variability, spectral variability and time lags between flux variations at different wavebands play an important role to understand the radiation and variation mechanism and physical structure of AGNs (See Wagner & Witzel 1995; Ulrich, Maraschi & Urry 1997, and reference therein).

3C 66A is classified as a low-frequency peaked BL Lac objects (LBL), according to the peak frequency of synchrotron emission (Padovani & Giommi 1995; Giommi et al. 1999). Long-term optical variability or optical spectral variability have been studied by lots of investigators (Fan & Lin 2000; D’Amicis et al. 2002; Vagnetti et al. 2003; Hu et al. 2006a): The study of Fan & Lin (2000) showed that the variability amplitude increased with frequency, and all these investigations showed the optical spectra turns bluer/flatter when the source brightens, although this tendency was strongly dependent on three data points in the study by Fan & Lin (2000), but this tendency was confirmed by many other authors (e.g., Gu et al. 2006; Dai et al. 2009; Rani et al. 2010). Short term variability and color variations have been investigated by many authors (e.g., Takalo et al. 1996; Gu et al. 2006; Rani et al. 2010): All their results showed short term variability, and the OJ-94 project on 3C 66A (Takalo et al.

Shao Ming Hu

Jianghua Wu

H. Y. Guo

X. Zhou

X. Zhang

Y. G. Zheng

¹Shandong Provincial Key Laboratory of Optical Astronomy and Solar-Terrestrial Environment, Shandong University at Weihai, 180 Cultral West Road, Weihai, Shandong, 264209, China Email: husm@sdu.edu.cn

²Max-Planck Institute for Extraterrestrial physics, Munich, 85741, Germany

³National Astronomical Observatories of Chinese Academy of Sciences, Beijing, 10012, China

⁴School of Computer Science, Harbin Institute of Technology at Weihai, Weihai, China

⁵Department of Physics, Yunnan Normal University, Kunming, Yunnan, China

1996) showed many intensive light curves; Significant positive correlation between V-I index and R magnitudes was detected by Gu et al. (2006); Significant positive correlation between V-R, R-I indices and V magnitudes were shown by Rani et al. (2010) but not for the other two color indices. Intra-day variability has also been previously reported by Carini & Miller (1991), Takalo et al. (1996) and De Diego et al. (1997), but some observations did not reveal intra-day variability (see Miller & McGimsey 1978; Takalo et al 1992; Xie et al. 1992). 3C 66A has been intensively monitored by two WEBT (Whole Earth Blazar Telescope) campaigns (see Böttcher et al. 2005, 2009). The first WEBT campaign was from 2003 July through 2004 April. Their results revealed intra-day variability within a 2-hour time-scale. During this campaign their study indicate a positive hardness-intensity correlation for low optical fluxes, which did not persist at higher state. B-R color index seemed to reach its minimum values several days prior to the B and R flux peaks. The second WEBT campaign covered the autumn and winter of 2007–2008. Evidence of rapid intra-day variability was revealed. There was no systematic spectral variability in the high state ($R \leq 14.0$) detected in this campaign, and there was no evident time lags among different optical bands by their analysis.

In order to investigate the variability, spectral variability and the time lag properties of this object, we monitored 3C 66A with BATC 60/90cm Schmidt telescope from 2005 January 26 to 2008 October 16. The observations and data reduction are described in section 2, the variability, optical spectral variability properties and time lags are presented in section 3, and section 4 gives a summary and discussion.

2 Observations and data reduction

Observations were carried out with a 60/90cm f/3 Schmidt telescope, which is located at Xinglong Station of National Astronomical Observatories of China. Images were recorded by a Ford Aerospace 2048 × 2048 CCD camera, mounted at the focus plane before the early of 2006. The pixel size of this CCD is 15 microns and the field of view is $58' \times 58'$, resulting in a resolution of $1.7''/\text{pixel}$. A new E2V 4096 × 4096 CCD was in commission from the early of 2006. The pixel size of the new CCD is 12 microns, so it results in a spatial resolution of $1.3''/\text{pixel}$. The telescope is equipped with a 15-colour intermediate-band photometric system, covering a wavelength range of 3000–10000 Å. The telescope and the photometric system are mainly used to carry out the BATC survey (Zhou 2005). From 2005 January

26 to 2006 November 23, observations of 3C 66A were performed with the BATC e, i and m bands in cyclic mode, whose central wavelengths are 4485Å, 6685Å and 8013Å, respectively. After that it was observed with BATC c, i and o filters in cyclic mode, so most of our observations are in c, i, and o bands. The central wavelengths of c and o band are 4206Å and 9173Å, respectively. The field of view of the central 512×512 pixels is large enough to cover the object and its comparison stars, so only the central 512×512 pixels are read out for blazar monitoring to shorten the readout time. For a good compromise between photometric precision and temporal resolution, we took 30–600 seconds as the exposure time for different filters, according to the weather condition and moon phase.

All images were processed with a pipeline data reduction procedure including bias subtraction, flat fielding, position calibration, aperture photometry and flux calibration. The adopted aperture was $8''$. The inner and outer radii of sky annulus were set to $9.1''$ and $13''$, respectively. Comparison stars A, B, C1 and C2 (from González-Pérez, Kidger & Martín-Luis 2001) were used for differential photometry during the data reduction. Their BATC magnitudes were obtained by observing them and three BATC standard stars, HD 19445, HD 84937 and BD+17d4708 on photometric nights. The BATC magnitudes of the standard stars were described by Yan et al. (2000). The extinction coefficients and zero points were obtained by the observations of these three standard stars, then the instrument magnitudes of the comparison stars were transferred to BATC magnitudes. These magnitudes and their errors were listed in Table 1. During the calibration, the instrumental magnitudes of 3C 66A and all the comparison stars were extracted first, then the object brightness was calculated to be the average of differential photometry magnitudes of the object relative to comparisons A, B and C1. C2 was chosen as the check star, which was used to verify the accuracy of our measurements. For each image, the difference between the instrumental magnitude of C2 and the average instrumental magnitude of A, B, and C1 was obtained, then the difference between this value and its average over the whole night was defined as S_x (x indicates the BATC band c, e, i, m and o.) for quantifying the accuracy of the measurements. The details on data reduction were described by Yan et al. (2000), Zhou et al. (2003) and references therein. The BATC magnitudes can also be transferred to standard Johnson-Cousins magnitudes by the relations obtained by Zhou et al. (2003). Covering four years from 2005 January 26 to 2008 October 16, 3C 66A was observed on 89 nights, during which observation time ranged from half an hour to 6 hours from night

to night, because of weather condition or other observation projects. In order to keep the accuracy of the following study, all the observations with photometry error bigger than 0.05 mag were discarded, so the error bars of the magnitude were not plotted in the following figures for clarity. Finally, 1994 observations from BATC were produced. All the observations are listed in Table 2, which gives an example of the photometry results in print version. Complete content is only available in electronic version. The universal date of observations (Col. 1) is followed by the universal time at the middle of exposure (Col. 2), Julian date at the middle of exposure (Col. 3), BATC band (Col.4), exposure time (Col. 5), BATC magnitude corresponding to the BATC band (Col. 6), photometry error E_x (Col. 7) and S_x , which indicates the confidence of the observation (Col. 8).

3 Variability and color variability

Variability and intra-day variability were analysed in detail using these observations. Color indices variability and time lags were studied adding the data taken and assembled by WEBT (Böttcher et al. 2005). Part of our observations overlapped with the second WEBT campaign on this source; the light curves during the overlapped period have been shown in Fig. 2 in Böttcher et al. (2009), and the variation agreed with the observations of WEBT campaign. But no comprehensive analysis was done on these data, because the BATC photometry filters are different from the filter system used by other participators.

3.1 Variability

Fig. 1 shows the light curves of 3C 66A in the BATC e, i and m bands from 2005 January 26 to 2006 November 23, and Fig. 2 shows the light curves of 3C 66A in c, i and o bands from 2006 November 26 to 2008 October 16. The narrower panels below the light curves present the variation of S_x , which indicates the confidence of the observations. One can see that all of them are less than 0.1 mag, and most of them are within 0.05 mag, which is almost at the same level as the photometry errors. Large amplitudes of variation were detected in our monitoring; the variation amplitude is 0.731, 0.792, 0.799 mag in e, i, and m band in Fig. 1, respectively. A big burst occurred during the second monitoring phase, and lots of fast oscillations are superimposed on the long term burst. The variation magnitude is 1.231, 1.406, 1.087 mag in c, i and o band, respectively, but it is a pity we could not monitor it during the two gaps

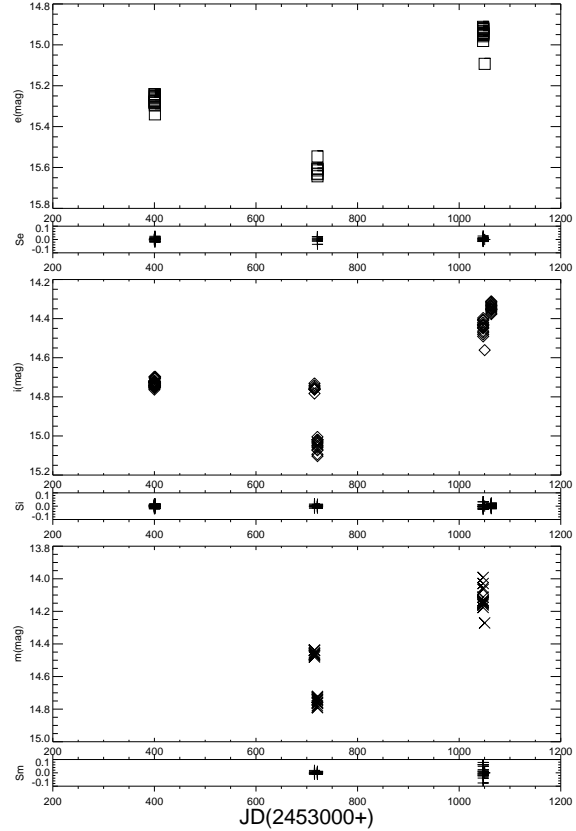


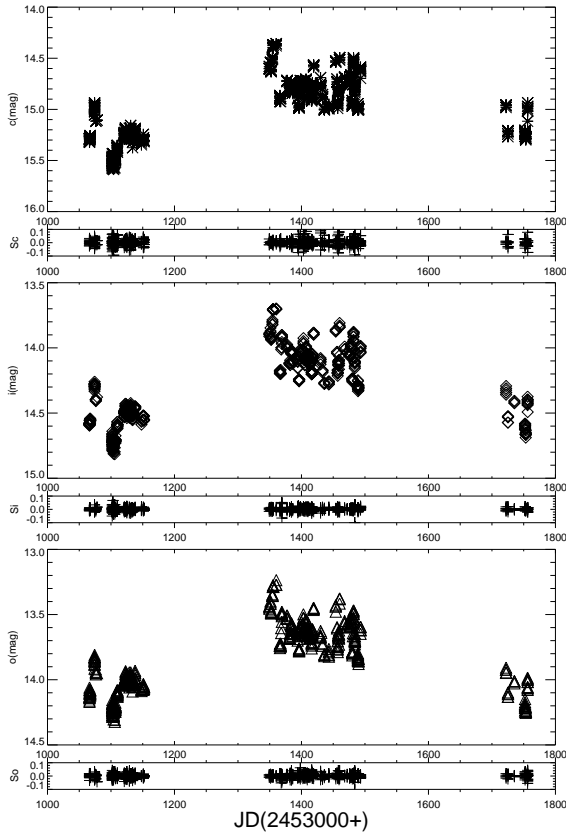
Fig. 1 Light curves of 3C 66A in BATC e, i and m bands from 2005 January 26 to 2006 November 23. The squares, diamonds and crosses show the light curve in e, i and m band, respectively. Plus signs in the narrow panels plot the deviation of S_x .

Table 1 BATC magnitudes and errors of the standard stars.

Band	A	B	C1	C2
c	14.060±0.013	16.020±0.037	12.865±0.011	15.497±0.025
e	13.810±0.010	15.157±0.018	12.854±0.009	14.581±0.013
i	13.516±0.009	14.389±0.013	12.932±0.008	13.741±0.010
m	13.463±0.012	14.164±0.017	12.998±0.010	13.484±0.013
o	13.468±0.014	14.027±0.020	13.003±0.012	13.382±0.015

Table 2 Photometry results.

Date(UT)	Time(UT)	JD	Band	Exp	Mag	E_x	S_x
yyyymmdd	hh:mm:ss.s	(day)		(s)	(mag)	(mag)	(mag)
20061126	14:01:56.0	2454066.08468	c	240	15.292	0.022	-0.024
20050129	10:43:15.0	2453399.94670	i	180	14.742	0.018	0.002
20061126	14:26:02.0	2454066.10141	o	240	14.128	0.033	-0.002
20050129	10:38:01.0	2453399.94307	e	300	15.241	0.036	-0.002
20051210	15:19:35.0	2453715.13860	m	450	14.437	0.018	-0.010

**Fig. 2** Light curves of 3C 66A in BATC c, i and o band from 2006 November 26 to 2008 October 16. The asterisks, diamonds and triangles demonstrate the light curve in c, i and o band, respectively. Plus signs in the narrow panels show the deviation of S_x .

because of the observing season or other observation projects.

The monitoring lasted several hours on many nights, which provided us a good opportunity to study the intra-day variability for 3C 66A. We took the criterion presented by Jang & Miller (1997) to quantitatively claim whether the object was variable or not within one night. They defined a parameter C as $C = \sigma_T / \sigma$, where σ_T is the standard deviation of the light curve, and σ is the standard deviation of S_x . Because S_x presents the variation of the comparison stars, σ can describe the confidence of the observations better. C is taken as the confidence parameter of variability. The source will be claimed to be variable at 99% confidence level when $C \geq 2.576$. We will say the object is variable only when $C \geq 2.576$ at least in two bands during one night if it was monitored in three or more bands (Jang & Miller 1997; Stalin et al. 2006). All the intra-night light curves continuously observed longer than 2 hours in the same band within the same night were analyzed, and all the results were listed in Table 3. The observation universal date (Col. 1) is followed by the BATC band (Col. 2), number of observations (Col. 3), the duration of the light curve in unit of hour (Col. 4), the value of C as defined above (Col. 5), and a label which indicates the source variable (1) or not (0) according to the criteria described above (Col. 6). The variability amplitude reached 0.1mag and even to 0.2mag on a few nights, but according to the criteria by Jang & Miller (1997), no intra-day variability was claimed on these 15 nights in our campaign. The same result has been reported by Miller & McGimsey (1978), Takalo et al (1992) and Xie et al. (1992) in their observations, but De Diego et al. (1997) have detected rapid intra-day variability in the infrared band.

Table 3 Intra-day variability analysis results.

Date	Band	N	H(h)	C	V/N
20061107	e	17	3.5	1.560	0
20061107	i	17	3.5	1.644	0
20061107	m	17	3.6	1.063	0
20061126	c	12	2.7	0.819	0
20061126	i	14	3.1	1.411	0
20061126	o	14	3.1	2.399	0
20061127	c	12	2.4	1.431	0
20061127	i	12	2.4	1.397	0
20061127	o	12	2.4	1.642	0
20061204	c	14	3.3	0.958	0
20061204	i	15	3.3	1.388	0
20061204	o	17	3.7	1.581	0
20070101	c	24	5.6	1.122	0
20070101	i	24	5.6	2.078	0
20070101	o	24	5.6	1.887	0
20070102	c	22	5.7	1.283	0
20070102	i	22	5.7	1.408	0
20070102	o	22	5.7	1.870	0
20070103	c	18	5.5	0.621	0
20070103	i	18	5.5	1.682	0
20070103	o	18	5.5	1.427	0
20070106	c	12	4.9	0.943	0
20070106	i	13	5.2	1.281	0
20070106	o	13	5.2	1.669	0
20070109	c	17	5.0	1.161	0
20070109	i	17	5.0	1.148	0
20070109	o	17	5.0	1.395	0
20070120	c	17	3.9	1.139	0
20070120	i	17	3.9	1.357	0
20070120	o	17	3.9	0.894	0
20070122	c	13	2.8	0.491	0
20070122	i	13	3.1	2.111	0
20070122	o	13	3.1	1.946	0
20070124	c	15	3.3	1.103	0
20070124	i	15	3.3	1.852	0
20070124	o	15	3.3	1.119	0
20071010	c	13	2.1	0.576	0
20071010	i	13	2.1	0.808	0
20071010	o	13	2.1	0.774	0
20080118	c	13	3.4	0.860	0
20080118	i	13	3.4	0.722	0
20080118	o	13	3.4	0.668	0
20080123	c	14	3.8	1.048	0
20080123	i	14	3.7	2.328	0
20080123	o	14	3.7	2.241	0

3.2 Spectral variability

The correlation between the brightness and the spectral shape (color index can be used to trace it in the optical band) of blazars has been investigated by many authors. Some research showed that the spectral shape became flat when the brightness increased, such as results of BL Lac from Racine (1970) and Vagnetti et al. (2003), result of OJ 287 from Gear, Robson & Brown (1986). But the opposite correlation has also been reported (e.g., Ramirez et al. 2004, for PKS 0736+017). Gu et al. (2006), Hu et al. (2006a), and Rani et al. (2010) showed that this relation may be different for different subclasses of blazar. Böttcher et al. (2005) concluded the correlation was different when the source was in different states. Villata et al. (2004) and Hu et al. (2006b) claimed the correlation level was different on different time-scale. The observation strategy of this 4-year monitoring can produce dense observations in different bands, which makes it possible to calculate the quasi-simultaneous color index to analyse the color variability and the correlation between brightness and color indices.

In order to study the color variability of 3C 66A, observations in the c and i bands were chosen. WEBT has made huge contributions to the study of blazars (e.g., Raiteri et al. 2007, 2008; Villata et al. 2009, and references therein). The optical observations in B and R bands of the extensive monitoring of the first WEBT campaign (Böttcher et al. 2005) were also used for the analysis in this paper. We chose observations in these bands because they were the most densely sampled bands in these two campaigns. Color indices were calculated using different band magnitudes taken within 30 minutes, and most of them are within 15 minutes. The error of the color index was calculated according to the rules of error propagation. The relation between the brightness and the color indices is demonstrated in Fig. 3. The correlation between c and c-i color index in the BATC campaign is given in the left four panels, and the right four panels show the correlation between B and B-R color index in the WEBT campaign. The top two panels illustrate the long term correlation covering each whole campaign, but the bottom six panels display the short flares identified from the long term light curves. The solid lines are the best Peterson linear fit. The fitted line slope b , which is taken as the color variability indicator, the error of b , the linear correlation coefficient r and the probability that r is zero are given in each panel. The observation time interval of each panel is labeled at the bottom of each panel. A positive correlation between brightness and the color index is found for all cases. The value of b for the BATC long

term light curve is 0.094, and those for the three short flares are 0.217, 0.153, 0.165. The value of b for the WEBT long term light curve and the three short flares are 0.061, 0.095, 0.122 and 0.113, respectively. The probability that r is zero for each linear fit is less than 0.03. We can see that the color variability indicators of the short flares are all larger than that of long term light curve. The result is the same if we discard the observations in the high state ($R \leq 14.0$) (see Sec. 3 of Böttcher et al. 2005) in the WEBT campaign, because the difference of b value is very small. So we conclude that the color variability indicator is larger on shorter time-scale for 3C 66A. This kind of tendency has been reported by Villata et al. (2004) and Hu et al. (2006b) for BL Lac.

3.3 Time lag

It can be seen that the shape of the light curves of c , i and o are in agreement with each other, so the z -transform discrete correlation function (ZDCF, Alexander 1997) was applied to the light curves. The ZDCF was used here as an estimation of the cross correlation function to calculate the time lags between different light curves. It applies z transformation to the correlation coefficients and uses equal population bins rather than the equal time bins in discrete correlation function (DCF, Edelson & Krolik 1988). One advantage of this technique is that it allows direct estimation of the uncertainties on the lag without more assumption-dependent Monte Carlo simulations. It has been shown in practice that the calculation of the ZDCF is more robust than that of the DCF when applied to sparsely and unequally sampled light curves (e.g., Edelson et al. 1996; Roy et al. 2000). The whole BATC campaign data can be used to detect the time lag, but the bump of the ZDCF curve is very wide and it is hard to claim a short time lag, because there are several big gaps in the monitoring. We analyzed the time lag between different optical bands with more continuous observations during two periods, one is from JD 2454066 to 2454153 (jd1), another is from JD 2454349 to 2454494 (jd2). The results are shown in Fig. 4. The top two panels display the ZDCF between the light curve of o and c , the second two panels from the top show the ZDCF between o and i , the third two panels from the top illustrate the ZDCF between i and c and the bottom two panels show the translated light curves of c , i , o band, whose brightness variation corresponds with each other. The left panels and right panels display the results of jd1 and jd2, respectively. All the results are listed in Table 4, $ZDCF_p$ is the peak value of ZDCF, τ_p is the time lag corresponding to $ZDCF_p$,

τ_G is the time lag corresponding to the center of the best gauss fit of the central part of ZDCFs and time lags, and Lag (last column) is the average of τ_p and τ_G . Time lags from jd1 are in the same level with those by Böttcher et al. (2009), But we can not get a consistent result from jd2.

Fig. 5 shows the c and i light curves and the color index variation curve. While the variation of c is consistent with the variation of i , the long term color index variation does not show a strong correlation with the light curves by the discrete correlation function (Edelson & Krolik 1988) analysis. But the minimum of the color index precedes the peak of the light curve by 2.07 days during the short flare from JD 2454106 to 2454152. The result is illustrated on the top panels of Fig. 6. This precedence could not be seen obviously in Fig. 5 because of the sparse and discontinuous observations during our campaign, so continuous observations by many telescopes located at positions with different longitude and latitude are crucial to study the spectral variation of blazars. The DCF analysis result was noisy and did not show a strong correlation between c - i and c during this flare; but the Gauss fit was applied to the bump of DCF, and the fitted center is -0.63 ± 3.84 day, which implies that the color index precedes the light curve of c band. This result agree with the result by Böttcher et al. (2005), and two short flares from Böttcher et al. (2005) are illustrated in Fig. 6. The middle panels show the result of the flare from JD 2454930 to 2454950 and the bottom panels display the flare from JD 2454820 to 2454850. The B-R color index precedes the light curve of B band by 4.16 and 2.99 days, respectively. DCF analysis was also applied to these two flares; both of the peaks of DCF are higher than that of BATC because of denser and more continuous sampling. The lags are -1.0 and -4.0 days corresponding to the peak of the DCF, and the gauss fitted centers are -2.06 ± 0.66 , -1.2 ± 1.16 days, which indicates that B-R precedes B. In other words, the optical spectra harden to the bluest state before it reaches to the brightest state. It maybe relates to the physical process of outburst.

4 Summary and discussion

3C 66A was monitored by the 60/90cm Schmidt telescope from 2005 January 26 to 2008 October 16 on 89 nights; 1994 observations in 5 BATC bands were obtained. Intra-day variability was analysed by the criteria presented by Jang & Miller (1997) on 15 nights, on which the duration of observations in all three bands

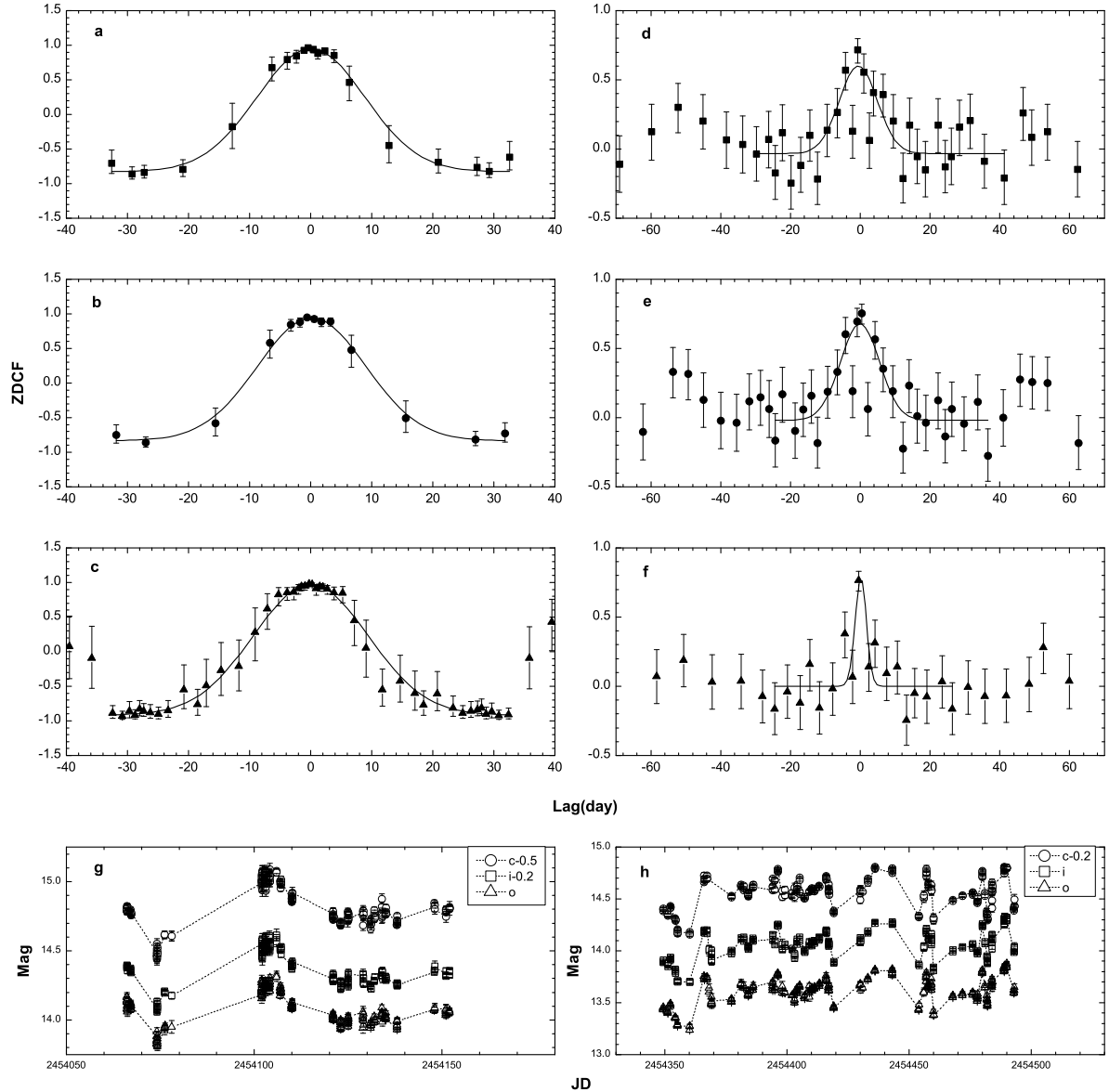
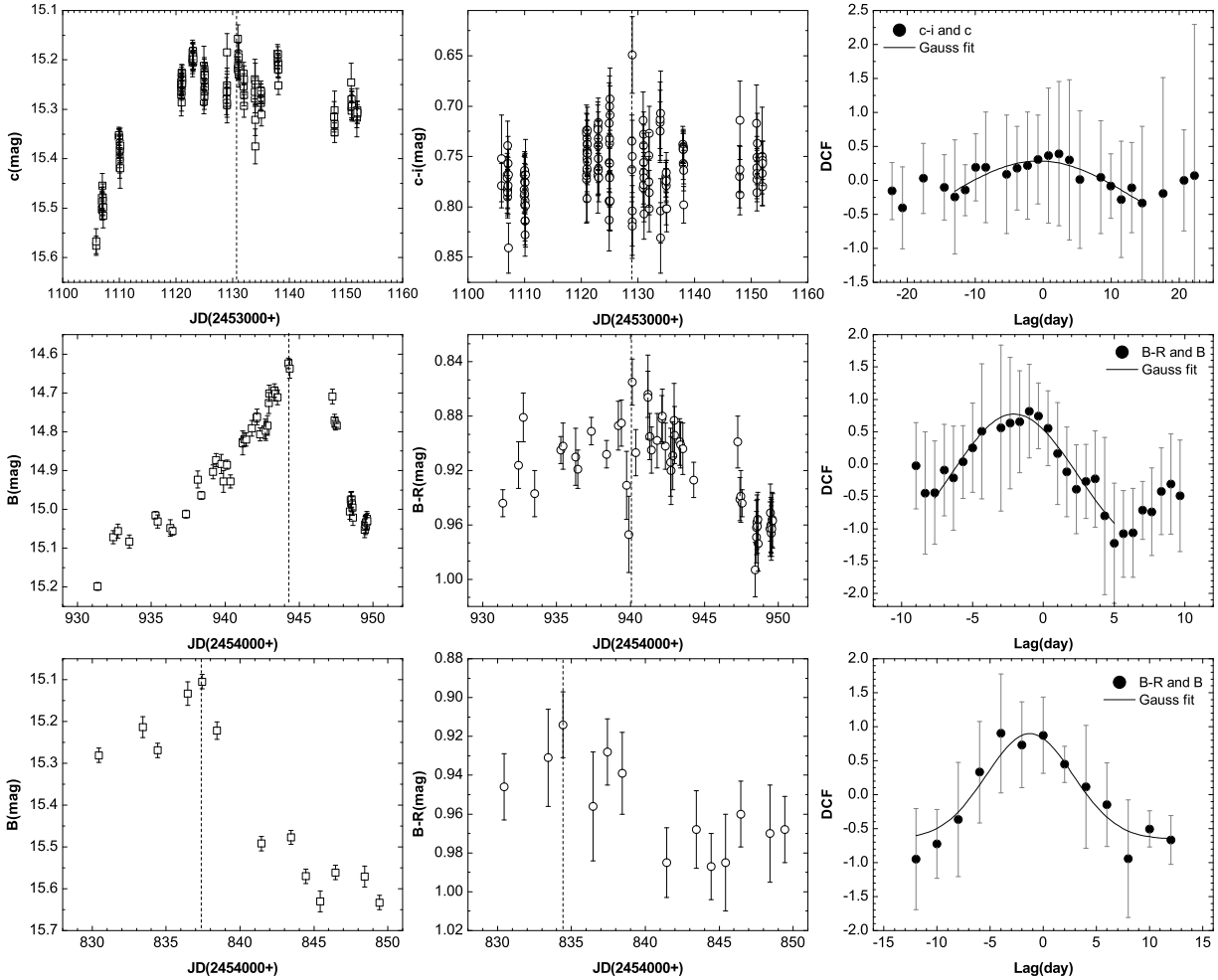


Fig. 4 Time lags between flux variations at different optical bands by ZDCF. Positive lag means long wavelength emission precedes that of short wavelength. Filled squares display the time lag between the light curve of o and c, filled circles show the ZDCF between i and c, and filled triangles illustrate the ZDCF between o and i. Panels a, b, c, g illustrate the result of jd1, and panels d, e, f, h display the results of jd2. Solid lines are the best gauss fit for the central part of data. The bottom two panels display the light curves.

Table 4 Time lags between flux variations at different optical bands by ZDCF.

Period	Bands	$ZDCF_p$	$\tau_p(\text{day})$	$\tau_G(\text{day})$	Lag(day)
jd1	o-c	0.960	$-0.386^{+0.136}_{-0.364}$	0.086 ± 0.439	-0.150
jd2	o-c	0.716	$-0.664^{+0.414}_{-0.336}$	-0.608 ± 0.986	-0.636
jd1	i-c	0.979	$-0.250^{+0.126}_{-0.210}$	0.049 ± 0.259	-0.101
jd2	i-c	0.765	$-0.371^{+0.621}_{-0.629}$	0.333 ± 0.602	-0.019
jd1	o-i	0.947	$-0.550^{+0.300}_{-0.450}$	0.190 ± 0.494	-0.180
jd2	o-i	0.753	$0.392^{+0.608}_{-0.642}$	-0.104 ± 0.868	0.144

**Fig. 6** The time lag between the color index and the brightness. Negative time lag means color index variation precedes the variation of light curve. Squares and circles display the light curve of $c(B)$ and the color variability of $c-i(B-R)$, respectively. Filled circles plot the time lag between the color index $c-i(B-R)$ and the magnitude $c(B)$. The solid lines are the best gauss fit, and the dash lines label the peak of the curves.

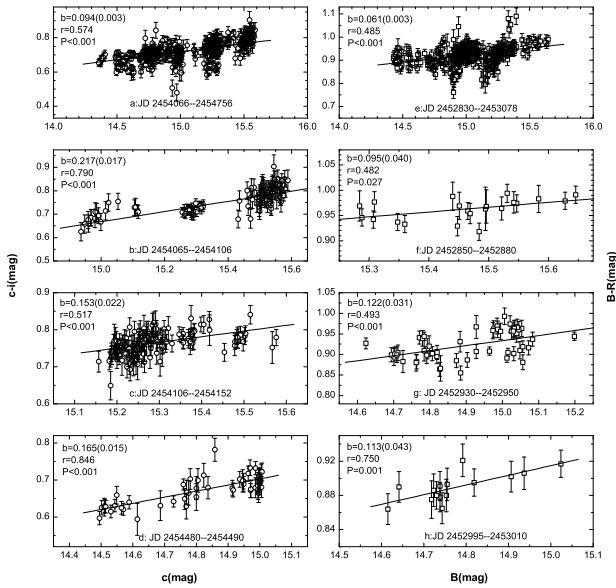


Fig. 3 The correlation between the color index and the brightness. Circles in the left four panels display the relationship between c and $c-i$, and squares in the right four panels show the correlation between B and $B-R$. The solid lines are the best linear fit. The errors of c and B are less than 0.05 and 0.08 mag, respectively, and they are not plotted for clarity.

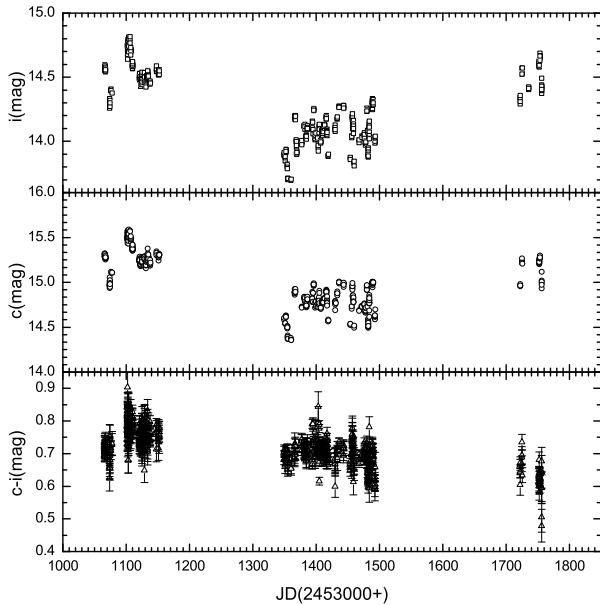


Fig. 5 The light curves and the color index light curve. Squares, circles and triangles illustrate the variation of i , c and $c-i$, respectively.

were longer than 2 hours, but no intra-day variability was claimed. One long term burst occurred during our monitoring; the variability amplitudes in c , i and o band are 1.231, 1.406, 1.087 mag, respectively. The profile of the light curves in three bands are consistent with each other, and time lags between different light curves were analyzed by ZDCF (Alexander 1997). The results from $jd1$ are consistent with those obtained by Böttcher et al. (2009). The spectral variability was studied on long term, and short flare time-scale; the results show that the spectrum turns bluer/flatter when the source turns brighter. Some models (Chiang & Bottcher 2002; Wang & Kusunose 2002) state that spectra of blazars become flat when they turn bright. The spectral variability indicator is bigger on shorter time-scale; this phenomenon may provide a constrain on the spectral variability mechanism. The interesting result that the minimum of the color index precedes the maximum of brightness by a few days was also detected in this paper. This means the optical spectra harden to the bluest state before a major outburst.

In the unified scheme of AGNs, blazars are thought to have the jet structure well-aligned with our line of sight (Antonucci 1993), and the jet is believed to originate and be accelerated by the central super-massive black hole surrounded by an accretion disk. Two broad, well-defined components of the blazar non-thermal dominated spectrum can be identified. The low-energy emission is commonly explained by synchrotron emission from non-thermal electrons in a relativistic jet (Konigl 1981). Many models have been proposed to explain the high-energy component; they can be roughly divided into leptonic or hadronic in origin, depending on whether it is electrons or protons which are responsible for the high-energy emission. While there are some hadronic models, which invoke protons as the ultimate source of high-energy emission (see Mücke et al. 2003; Böttcher 2007, and references therein), the majority of the proposed models are leptonic models, which assume the high-energy emission comes from inverse Compton scattering of relativistic electrons on some low-energy seed photons. The source of the seed photons is still an open question and many possible origins have been involved, such as internally produced synchrotron photons (Synchrotron Self-Compton, see Jones, O’dell & Stein 1974; Marscher & Travis 1996), photons from an external source, such as accretion disk or diffuse isotropic photons coming from broad line clouds (External Compton, see Dermer, Schlickeiser & Mastichiadis 1992; Sikora et al. 2001; Celotti et al. 2008), or combinations thereof (Dermer, Sturmer & Schlickeiser 1997).

Based on our observational results, we think the variability and the optical color variation could be reasonably explained by shock-in-jet models that involve relativistic shocks propagating outwards (e.g., Marscher & Gear 1985; Wagner & Witzel 1995), and which was discussed by Rani et al. (2010). The larger flares are expected to be produced by the emergence and motion of a new shock triggered by some strong variation in a physical quantity such as velocity, electron density or magnetic field moving into and through the relativistic jet. Smaller variations may be nicely explained by turbulence behind a shock propagating down the jet (Marscher et al. 1992). So jet models can produce different variability at different colors. In the usual boosted synchrotron models involving shocks propagating down the jets (e.g., Marscher & Gear 1985; Marscher et al. 2008), radiation at different frequencies is produced at different distances behind the shocks. Typically, higher frequency photons emerge and stop sooner (Valtaoja et al. 1992, 2002). This maybe introduces the result that the bluest state precedes the maximum of brightness. And we expect to see time lag which shows high frequency flux precedes that of low frequency. This kind of time lag was detected by us even not in all cases. During the early phase of a rise in flux, one is more likely to see a bluer color. However, later observation during the same flare might show a more enhanced redder band as the bluer one might have stopped rising or may even have passed its peak. 3C 66A is a typical BL Lac object, whose flux is completely dominated by jet. The former situation should be more likely to be seen than the latter, yielding a predominance of bluer-when-brighter situations which was shown by our observations. The geometry of the jet may also affect the flux. The direction of the jet varies, which leads to the variability triggered by the variation of Doppler factor, as the knots move relativistically on helical trajectories within a small angle with respect to the observer. This may produce the long-term mildly chromatic variability (Villata et al. 2004; Hu et al. 2006b), while the intrinsic shock-in-jet mechanism may give a stronger chromatic short term variability. This scenario can explain the result that the spectral variability indicator is bigger on shorter time-scale. So we suggest the intrinsic shock-in-jet mechanism adding geometric effects may be the model of the variability of 3C 66A. More dense and long term simultaneous multi-color observations and studies should be carried out to understand and constrain the radiation mechanism well.

Acknowledgments

We thank the anonymous referee for numerous suggestions that helped to improve this paper. We owe great thanks to all the BATC staffs who make great efforts to the observations. We are also grateful to Ralf Bender, Frank Grupp and Anne Bauer for helpful discussion and revision. This research is supported by the National Natural Science Foundation of China and Chinese Academic of Sciences joint fund on astronomy under project No. 10778619, 10778701 and the foundation of Shandong university at Weihai (No. 2010ZRYB003, 20080030). This work is partly supported by Max-Planck Institute for Extraterrestrial physics, University Observatory of the Ludwig-Maximilians University. This research has made employment of WEBT data and the NASA/IPAC Extragalactic Database (NED). Jianghua Wu and X. Zhou are supported by the Chinese National Natural Science Foundation grants 10633020, 10778714, and 11073032.

References

- Alexander T., 1997, in *Astronomical Time Series*, Eds. D. Maoz, A. Sternberg, E.M. Leibowitz (Dordrecht: Kluwer), 163
- Antonucci R., 1993, *Annu. Rev. Astron. Astrophys.*, 31, 473
- Bauer A. et al., 2009, *Astrophys. J.*, 699, 1732
- Böttcher M. et al., 2005, *Astrophys. J.*, 631, 169
- Böttcher M., 2007, *Astrophys. Space Sci.*, 309, 95
- Böttcher M. et al., 2009, *Astrophys. J.*, 694, 174
- Carini M. T., Miller H. R., 1991, *Bull. Am. Astron. Soc.*, 23, 1420
- Celotti A., Ghisellini G., 2008, *Mon. Not. R. Astron. Soc.*, 385, 283
- Chiang J., Böttcher M., 2002, *Astrophys. J.*, 564, 92
- Dai B. Z. et al., 2009, *Mon. Not. R. Astron. Soc.*, 392, 1181
- D'Amicis R., Nesci R., Massaro E., Maesano M., Montagni F., D'Alessio F., 2002, *Publ. Astron. Soc. Aust.*, 19, 111
- De Diego J. A., Kidger M. R., González-Pérez N., Lehto H., 1997, *Astron. Astrophys.*, 318, 331
- Dermer C. D., Schlickeiser R., Mastichiadis A., 1992, *Astron. Astrophys.*, 256, L27
- Dermer C. D., Sturmer S. J., Schlickeiser R., 1997, *Astrophys. J. Suppl. Ser.*, 109, 103
- Edelson R. A., Krolik J. H., 1988, *Astrophys. J.*, 333, 646
- Edelson R. A. et al. 1996, *Astrophys. J.*, 470, 364
- Fan J. H., Lin R. G., 2000, *Astrophys. J.*, 537, 101
- Gear W. K., Robson E. I., Brown L. M. J., 1986, *Nature*, 324, 546
- Giommi P. et al., 1999, *Astron. Astrophys.*, 351, 59
- González-Pérez J. N., Kidger M. R., Martín-Luis F., 2001, *Astron. J.*, 122, 2055
- Gu M. F., Lee G.-U., Pak S., Yim H. S., Fletcher A. B., 2006, *Astron. Astrophys.*, 450, 39
- Gupta A. C., Banerjee D. P. K., Ashok N. M., Joshi U. C., 2004, *Astron. Astrophys.*, 422, 505
- Hatman R. C. et al., 1999, *Astrophys. J. Suppl. Ser.*, 123, 79
- Hu S. M., Zhao G., Guo H. Y., Zhang X., Zheng Y. G., 2006, *Mon. Not. R. Astron. Soc.*, 371, 1243
- Hu S. M., Wu J. H., Zhao G., Zhou X., 2006, *Mon. Not. R. Astron. Soc.*, 373, 209
- Jang M., Miller H. R., 1997, *Astron. J.*, 114, 565
- Jones T. W., O'dell S. L., Stein W. A., 1974, *Astrophys. J.*, 188, 353
- Konigl A., 1981, *Astrophys. J.*, 243, 700
- Landt H., Padovani P., Perlman E. S., Giommi P., 2004, *Mon. Not. R. Astron. Soc.*, 351, 83
- Maraschi L. et al., 1994, *Astrophys. J.*, 435, 91
- Marscher A. P., Gear W. K., 1985, *Astrophys. J.*, 298, 114
- Marscher A. P., Gear W. K., Travis J. P., 1992, in Valtaoja E., Valtonen M., eds, *Variability of Blazars*. Cambridge Univ. Press, Cambridge, p.85
- Marscher A. P., Travis J. P., 1996, *Astron. Astrophys. Suppl. Ser.*, 120, 537
- Marscher A. P. et al., 2008, *Nature*, 452, 966
- Miller H. R., McGimsey B. Q., 1978, *Astrophys. J.*, 220, 19
- Mücke A., Protheroe R. J., Engel R., Rachen J.P., Stanev T., 2003, *Astropart. Phys.*, 18, 593
- Padovani P., Giommi P., 1995, *Astrophys. J.*, 444, 567
- Racine R., 1970, *Astrophys. J.*, 159, L99
- Raiteri C. M. et al., 2007, *Astron. Astrophys.*, 473, 819
- Raiteri C. M. et al., 2008, *Astron. Astrophys.*, 491, 755
- Ramirez A., de Diego J. A., Dultzin-Hacyan D., Gonzalez-Perez J. N., 2004, *Astron. Astrophys.*, 421, 83
- Rani B. et al., 2010, *Mon. Not. R. Astron. Soc.*, 404, 1992
- Roy M. et al. 2000, *Astrophys. J.*, 545, 758
- Sikora M., Blazejowski M., Begelman M. C., Moderski R., 2001, *Astrophys. J.*, 554, 1
- Stalin C. S., Gopal-Krishna G.-K., Sagar Ram, Wiita Paul J., Mohan V., Pandey A. K., 2006, *Mon. Not. R. Astron. Soc.*, 366, 1337
- Takalo L. O., Kidger M. R., De Diego J. A., Sillanpää A., Nilsson K., 1992, *Astron. J.*, 104, 40
- Takalo L. O. et al., 1996, *Astron. Astrophys. Suppl. Ser.*, 120, 313
- Ulrich M.-H., Maraschi L., Urry C. M., 1997, *Annu. Rev. Astron. Astrophys.*, 35, 445
- Urry C. M., Padovani P., 1995, *Publ. Astron. Soc. Pac.*, 107, 803
- Vagnetti F., Trevese D., Nesci R., 2003, *Astrophys. J.*, 590, 123V
- Valtaoja E., Terasranta H., Urpo S., Nesterov N. S., Lainela M., Valtonen M., 1992, *Astron. Astrophys.*, 254, 80
- Valtaoja E., Savolainen T., Wiik K., Lähteenmäki A., 2002, *Publ. Astron. Soc. Aust.*, 19, 117
- Villata M. et al., 2004, *Astron. Astrophys.*, 421, 103
- Villata M. et al., 2009, *Astron. Astrophys.*, 501, 455
- Wagner S. J., Witzel A., 1995, *Annu. Rev. Astron. Astrophys.*, 33, 163
- Wang J.-M., Kusunose M., 2002, *Astrophys. J. Suppl. Ser.*, 138, 249
- Xie G. Z., Li K. H., Liu F. K., Wu J. X., Fan J. H., Zhu Y. Y., Cheng F. Z., 1992, *Astrophys. J. Suppl. Ser.*, 80, 683
- Yan H. J. et al., 2000, *Publ. Astron. Soc. Pac.*, 112, 691
- Zhou X. et al., 2003, *Astron. Astrophys.*, 397, 361
- Zhou X., 2005, *JKAS*, 38, 203